Generalized gradient approximation bridging the rapidly and slowly varying density regimes: A PBE-like functional for hybrid interfaces

Eduardo Fabiano,[1] Lucian A. Constantin,[2] and Fabio Della Sala[1,2]

[1]*National Nanotechnology Laboratory (NNL), Istituto di Nanoscienze-CNR, Via per Arnesano 16, I-73100 Lecce, Italy*
[2]*Center for Biomolecular Nanotechnologies (CBN), Italian Institute of Technology (IIT), Via Barsanti, I-73010 Arnesano, Italy*

We propose a generalized gradient approximation constructed for hybrid interfaces, which is based on the Perdew, Burke, Ernzerhof (PBE) functional form and interpolates between the rapidly PBE and slowly varying (PBEsol, the revised PBE for solid-state systems) density regimes. This functional approximation (named PBEint) recovers the right second-order gradient expansion of the exchange energy and is accurate for jellium surfaces, interacting jellium slabs, molecules, solids, and metal-molecule interfaces.

PACS number(s): 71.10.Ca, 71.15.Mb, 71.45.Gm

The modeling of hybrid interfaces, such as organic molecules on metal substrates, is of utmost importance to analyze and/or to engineer molecular and optoelectronic devices.[1,2] Despite recent progress in the theoretical understanding and description of these systems[3–8] conventional and/or preliminary calculations for large systems are always performed within the Kohn-Sham density-functional theory (DFT),[9] using conventional approximations to the exchange-correlation (xc) energy, such as the generalized gradient approximation (GGA).[10] Due to their simplicity, GGA functionals are computationally very efficient but for good numerical accuracy the satisfaction of exact xc energy properties is required.

The GGA form for exchange energy of a spin-unpolarized system is

$$E_x^{GGA}[n] = \int d\mathbf{r}\, n(\mathbf{r})\, \epsilon_x^{unif}[n(\mathbf{r})]\, F_x^{GGA}[s(\mathbf{r})], \qquad (1)$$

where ϵ_x^{unif} is the exchange energy per particle of the uniform electron gas, F_x^{GGA} is the exchange enhancement factor, and $s = |\nabla n|/(2k_F n)$ is the reduced density gradient which measures the variation in the electron density over a Fermi wavelength $\lambda_F = 2\pi/k_F$, with $k_F = (3\pi^2 n)^{1/3} = (9\pi/4)^{1/3}/r_s$ representing the magnitude of the local Fermi wave vector, and r_s is the local bulk parameter. (Unless otherwise stated, atomic units are used throughout, i.e., $e^2 = \hbar = m_e = 1$.) Recent work[11,12] showed that a GGA cannot be both accurate for atoms and solids. A GGA that is accurate for atoms should recover the asymptotic expansion of neutral atoms for large Z, $E_x = -0.2208 Z^{5/3} - 0.196 Z + \cdots$, where Z is the nuclear charge. This expansion is well described by the nonempirical Perdew-Burke-Ernzerhof (PBE) GGA functional, whose enhancement factor is

$$F_x^{GGA}(s) = 1 + \kappa - \frac{\kappa}{1 + \mu^{PBE} s^2/\kappa}, \qquad (2)$$

where $\mu^{PBE} = 0.2195$ and $\kappa = 0.804$ is fixed from the Lieb-Oxford bound.[10] The value of μ^{PBE} is almost twice larger than the one obtained from the second-order gradient expansion ($\mu^{GE} = 10/81$) (Ref. 13) that is exact in the slowly varying density regime. Thus, the PBEsol functional[12] was proposed for solids and surfaces, which recovers the gradient

expansion for exchange over a wide range of density gradients ($\mu^{PBEsol} = \mu^{GE}$). Several PBE-like approximations were constructed in the last decades,[14–19] however none of them was explicitly derived to achieve best accuracy for interfaces.

In this paper we propose a simple approximation (named PBEint) constructed for interfaces, by replacing in Eq. (2) μ^{PBE} with

$$\mu^{PBEint} = \mu^{GE} + (\mu^{PBE} - \mu^{GE}) \frac{\alpha s^2}{1 + \alpha s^2}. \qquad (3)$$

Our construction ensures that in the rapidly varying density regime $\mu^{PBEint} \rightarrow \mu^{PBE}$ and in the slowly varying density regime $\mu^{PBEint} \rightarrow \mu^{PBEsol}$. Note that with the choice of Eq. (3) we do not construct an explicit interpolation between PBE and PBEsol but rather connect smoothly the two density regimes. Nevertheless, the resulting exchange enhancement factor (see Fig. 1) smoothly varies between PBEsol, at small values of s (mostly needed for solids and surfaces), and PBE, at high values of s (needed for molecules). The second-order gradient expansion of the exchange energy is thus recovered by PBEint over a large range of reduced-gradient values ($s \leq 1$; see Fig. 1). The value of α was fixed to 0.197 from the constraint $d^2 F_x^{PBEint}(s)/d(s^2)^2|_{s=0} = 0$ that ensures a monotonic behavior of $dF_x^{PBEint}/d(s^2)$ (inset of Fig. 1) and a right sign of $d/ds[s^{-1} dF_x^{PBEint}/ds]$ (Ref. 20) for a smooth functional derivative $\delta E_x^{PBEint}/\delta n$. For the correlation functional we also used a PBE-like expression and replaced the value of
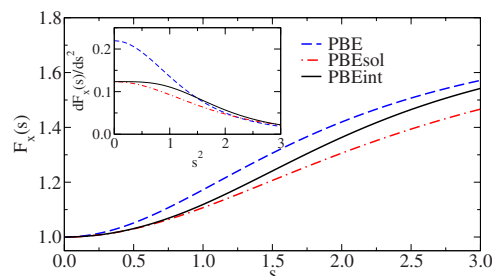

FIG. 1. (Color online) Exchange enhancement factor for PBE, PBEsol, and PBEint. Inset: derivative of the enhancement factor versus the squared reduced gradient s^2.
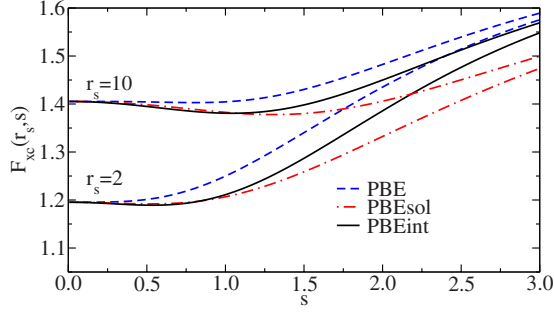
FIG. 2. (Color online) PBE, PBEsol, and PBEint xc enhancement factors F_{xc} for the spin-unpolarized case as a function of the reduced gradient s for $r_s=2$ and $r_s=10$.

FIG. 4. (Color online) PBEint and PBEsol wave-vector-resolved xc surface energies $\gamma_{xc}(k)$, versus $k/2k_F$ for jellium slabs of thicknesses $a=2.23\lambda_F$ and $r_s=2.07$ and $r_s=3$, respectively. Also shown are the exact initial slopes.

the second-order gradient expansion coefficient $\beta(r_s)$. In the PBE functional the high-density limit value $\beta(r_s \rightarrow 0) = \beta^{PBE}=0.06675$, calculated by Ma and Brueckner,[21] is used. In PBEsol the coefficient is empirical and fitted to jellium surfaces ($\beta^{PBEsol}=0.046$). Refitting jellium surfaces, we obtained $\beta^{PBEint}=0.052$, in between the previous values.

In Fig. 2 we show the xc enhancement factor $F_{xc}^{GGA} = \epsilon_{xc}^{GGA}(n,\nabla n)/\epsilon_x^{unif}(n)$ for two values of r_s. In the range $s \lesssim 1$ and $2 < r_s < 10$, which is the most important for densely packed solids, F_{xc}^{PBEint} is practically identical with F_{xc}^{PBEsol}. In the range $2 \lesssim s$ and $2 < r_s$, which is relevant for the description of atomic and molecular properties, PBEint shows a significantly larger nonlocality than PBEsol. Thus, we may expect PBEint to be accurate for solids and reasonably good for molecules.

As a first test to verify the accuracy of our GGA for interfaces, we performed a study at the exchange level for jellium interfaces. The interaction between two identical, thick jellium slabs at different distances can model a "nanogap" used in molecular electronic devices.[1] We chose two jellium slabs of thicknesses $2.75\lambda_F$ each, and we introduced and calculated the following relative errors:
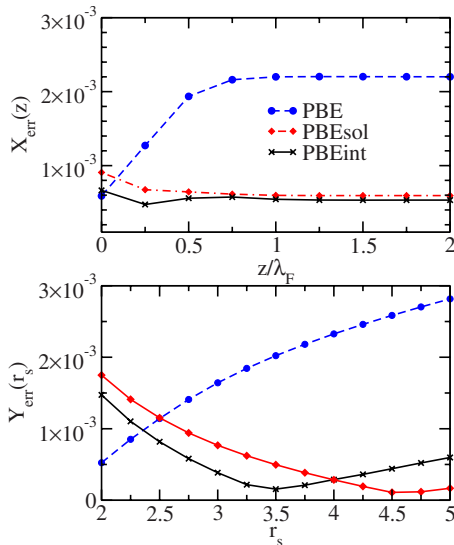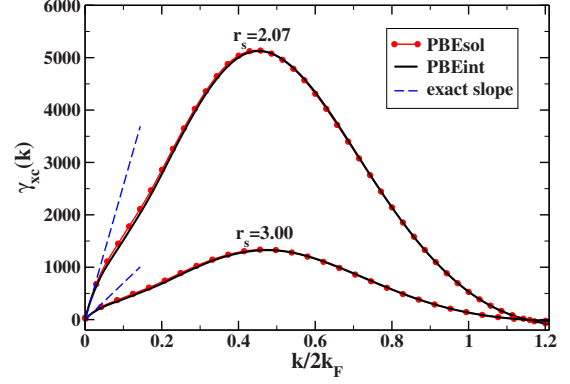

FIG. 3. (Color online) $X_{err}(z)$ (top panel) and $Y_{err}(r_s)$ (bottom panel) for PBE, PBEsol, and PBEint. See text for details.

$$X_{err}(z) = \frac{1}{5-2}\int_2^5 \left| \frac{E_x^{EXX}(z,r_s) - E_x^{GGA}(z,r_s)}{E_x^{EXX}(z,r_s)} \right| dr_s,$$

$$Y_{err}(r_s) = \frac{1}{2}\int_0^2 \left| \frac{E_x^{EXX}(z,r_s) - E_x^{GGA}(z,r_s)}{E_x^{EXX}(z,r_s)} \right| dz$$

with z the distance between the slabs in units of λ_F. The exact exchange (EXX) energy for two jellium slabs is computed as described in Ref. 22. The upper panel of Fig. 3 reports the $X_{err}(z)$ values for PBE, PBEsol, and PBEint. The quantity $X_{err}(z)$ describes how well, for a given z, the exchange energy is described averaging over jellium slabs with $2 < r_s < 5$. This is the range that includes most of the metals. PBE gives an error four times larger than PBEsol for $z > 0.5$, showing the importance of the second-order gradient expansion of the exchange energy for jellium interfaces. Note that for $z \approx 0$, PBE is as accurate as PBEint because of an error cancellation between the surface and bulk regions. The PBEint error is smaller than PBEsol one at all distances and provides support for the nonlocality of the enhancement factor shown in Fig. 1. The lower panel of Fig. 3 reports the corresponding $Y_{err}(r_s)$ values. The quantity $Y_{err}(r_s)$ describes how well, for a given r_s, the exchange energy is described averaging over different distances $0 < z/\lambda_F < 2$. For small r_s PBE gives the best results but then the error rapidly increases. PBEsol is the best in the low-density regime (high r_s). In the range $2.3 \le r_s \le 4$ PBEint is the most accurate approximation.

TABLE I. Jellium surface exchange-correlation energies (erg/cm^2) for PBE, PBEsol, PBEint, and the fixed-node diffusion Monte Carlo (DMC) calculations (Refs. 24 and 25).

r_s	PBE	PBEint	PBEsol	DMC
2	3265	3378	3374	3392 ± 50
3	741	774	774	768 ± 10
4	252	267	267	261 ± 8
6	52	56	56	52.5

TABLE II. Error statistics for PBE, PBEsol, and PBEint density functionals.

	PBE	PBEint	PBEsol
	Lattice constants (Å) of seven solids		
ME	0.070	0.036	0.008
MAE	0.070	0.040	0.026
	Bulk moduli B_0 (GPa) of seven solids		
ME	−8.79	−3.69	3.80
MAE	10.30	10.00	8.03
	AE6 atomization energies (kcal/mol)		
ME	11.588	23.863	34.898
MAE	14.565	24.780	34.898

In order to study in detail the behavior of PBEint at jellium surfaces, we constructed the xc hole that recovers the PBEint xc energy functional following the calculation described in Ref. [23]. We found that the numerical solution of $\mathcal{H}(s)$ can be fitted with the same analytic expression as PBEsol [see Eq. (14) of Ref. [23]], with parameters $a_1 = 1.9549 \times 10^{-8}$, $a_2 = 0.0143741$, $a_3 = 0.066962$, $a_4 = 0.000753$, and $a_5 = 0.012064$. The wave-vector-resolved xc surface energies $\gamma_{xc}(k)$ [defined in Eq. (17) of Ref. [23]] are shown in Fig. [4]; the jellium xc surface energies are reported in Table [I]. Inspection of the data shows that PBEint yields results as good as PBEsol. We recall that PBEsol can describe jellium surfaces at any wave vector with high accuracy.[23]

Then, we considered systems with real atoms, including: (i) bulk, (ii) molecules, and (iii) metal-molecule interfaces. The complete set of results, including accurate reference data, is reported in supplementary material;[26] here the main results are summarized and compared with the limiting cases PBE and PBEsol. (i) We computed equilibrium lattice constants and bulk moduli for a small but representative set of materials (simple metal: Na; transition metals: Ag, Pd, and Cu; semiconductors: Si and GaAs; and ionic solid: NaCl). Mean errors (MEs) and mean absolute errors (MAEs) are reported in Table [II]. The PBEint functional provides accurate results, not as good as PBEsol but almost twice as good as PBE. A similar trend is found for the bulk moduli. (ii) We computed atomization energies (at optimized geometries) for the AE6 set of molecules[27] (see Table [II]), which is a popular
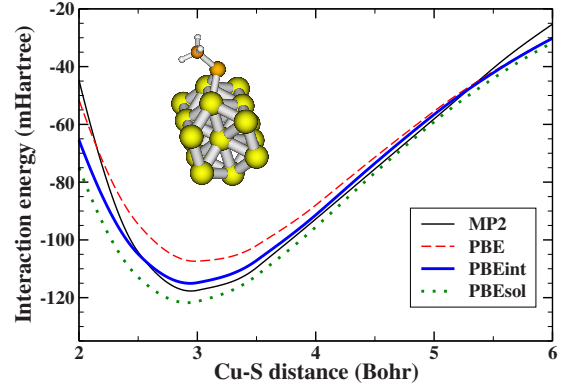
FIG. 5. (Color online) Interaction energy of the SCH_3 molecule on a Cu_{17} cluster as resulting from PBE, PBEint, and PBEsol calculations. MP2 results are also reported.

benchmark test set for DFT atomization energies. PBEint, although not reaching the accuracy of PBE, performs better than PBEsol and yields reasonably good atomization energies.

(iii) Finally, we considered model systems for real metal-molecule interfaces. We modeled the metal as a finite cluster. As shown in Ref. [8], differences between xc functionals are stable with respect to the cluster size. We focused our attention on the sulfur-copper interface and studied the interaction energy of phenylthiolate (PT), SCH_3, and SH molecules on copper clusters of 17 and 9 atoms. The adsorption of thiolated molecules on noble metals is in fact one of the most studied examples of metal-molecule interfaces,[5,28–30] and Cu is a simple model for noble metals.[31] Results are summarized in Table [III] for all systems and compared with MP2 calculations. The use of MP2, although it might result problematic for a metal because of the small highest occupied molecular orbital-lowest unoccupied molecular orbital gap, was found to provide accurate results for metal-molecule interactions when small and medium size metal clusters are considered.[29,30] In Fig. [5] we also report the full dissociation curve for the SCH_3 on Cu_{17}. PBEint provides a good description of the interaction energy, in close agreement with MP2, over a large range of Cu-S distances ($2.5 \leq r \leq 5.5$). Moreover it yields in general the best results for both the equilibrium distance and interaction energy at equilibrium. Note that for the considered systems, characterized by a covalent bond between the molecule and the substrate, dispersion interactions[7] are expected to play a minor role (also due to

TABLE III. Equilibrium distance R_0 (bohr) and interaction energy E_{int} (mhartree) of SCH_3 adsorbed on a Cu_{17} cluster, and PT and SH molecules on a Cu_9 cluster.

		PBE	PBEint	PBEsol	MP2
SCH_3-Cu_{17}	R_0	3.03	2.96	2.92	2.97
	E_{int}	107.36	114.82	121.32	118.46
PT-Cu_9	R_0	3.29	3.21	3.17	3.17
	E_{int}	92.77	102.78	109.83	102.01
SH-Cu_9	R_0	3.31	3.24	3.20	3.22
	E_{int}	86.76	97.88	105.14	92.70

the small size of the molecule). Thus, a direct comparison between GGA DFT and MP2 results can be performed.

In conclusion, we constructed a PBE-like functional which is much better than PBE for real solid-state systems, more accurate than PBEsol for molecular systems and better than both PBE and PBEsol for jellium-jellium and metal-molecule interfaces. We found that at a hybrid interface, in case of strong interactions like covalent bonds, the xc approximation must be accurate especially for the metal and its surface, and must have a stronger nonlocality than PBEsol GGA because of the significant variations in the density near the molecule. Our PBEint has all these features and is a promising tool for the study of hybrid surfaces.

Computational details. For solid-state calculations we used the FHI-AIMS program[32] with the light numerical basis set, scalar relativistic effects included through the zeroth-order relativistic approximation, and a $18 \times 18 \times 18$ k-point

grid. Results for PBE (PBEsol) agree with the ones in Ref. 33 with a MAE of 0.007 (0.009) Å.

For molecular and cluster calculations we used the TURBOMOLE program[34] and the def2-TZVPP Gaussian basis set.[35] The geometry of the SCH_3-Cu_{17} was obtained by cutting a fully optimized Cu (110) surface with adsorbed molecules.[31] For PT-Cu_9 and SH-Cu_9 a cluster extracted from a Cu (111) surface was combined with molecules in perfect perpendicular orientation.

[1] A. Nitzan and M. A. Ratner, Science **300**, 1384 (2003).

[2] S. Braun, W. R. Salaneck, and M. Fahlman, Adv. Mater. **21**, 1450 (2009).

[3] T. Klüner, N. Govind, Y. A. Wang, and E. A. Carter, Phys. Rev. Lett. **86**, 5954 (2001).

[4] H. Vázquez, F. Flores, R. Oszwaldowski, J. Ortega, R. Pérez, and A. Kahn, Appl. Surf. Sci. **234**, 107 (2004).

[5] G. Heimel, L. Romaner, J.-L. Brédas, and E. Zojer, Phys. Rev. Lett. **96**, 196806 (2006).

[6] J. B. Neaton, M. S. Hybertsen, and S. G. Louie, Phys. Rev. Lett. **97**, 216405 (2006).

[7] P. Sony, P. Puschnig, D. Nabok, and C. Ambrosch-Draxl, Phys. Rev. Lett. **99**, 176401 (2007).

[8] Q. M. Hu, K. Reuter, and M. Scheffler, Phys. Rev. Lett. **98**, 176103 (2007).

[9] W. Kohn and L. J. Sham, Phys. Rev. **140**, A1133 (1965).

[10] J. P. Perdew, K. Burke, and M. Ernzerhof, Phys. Rev. Lett. **77**, 3865 (1996).

[11] J. P. Perdew, L. A. Constantin, E. Sagvolden, and K. Burke, Phys. Rev. Lett. **97**, 223002 (2006).

[12] J. P. Perdew, A. Ruzsinszky, G. I. Csonka, O. A. Vydrov, G. E. Scuseria, L. A. Constantin, X. Zhou, and K. Burke, Phys. Rev. Lett. **100**, 136406 (2008).

[13] P. R. Antoniewicz and L. Kleinman, Phys. Rev. B **31**, 6779 (1985).

[14] Y. Zhang and W. Yang, Phys. Rev. Lett. **80**, 890 (1998).

[15] Z. Wu and R. E. Cohen, Phys. Rev. B **73**, 235116 (2006); **78**, 197102 (2008).

[16] Y. Zhao and D. G. Truhlar, J. Chem. Phys. **128**, 184109 (2008).

[17] B. Hammer, L. B. Hansen, and J. K. Norskov, Phys. Rev. B **59**, 7413 (1999).

[18] A. Ruzsinszky, G. I. Csonka, and G. E. Scuseria, J. Chem. Theory Comput. **5**, 763 (2009).

[19] L. S. Pedroza, A. J. R. da Silva, and K. Capelle, Phys. Rev. B **79**, 201106 (2009).

[20] J. P. Perdew and Y. Wang, Phys. Rev. B **33**, 8800 (1986).

[21] S.-K. Ma and K. A. Brueckner, Phys. Rev. **165**, 18 (1968).

[22] C. M. Horowitz, L. A. Constantin, C. R. Proetto, and J. M. Pitarke, Phys. Rev. B **80**, 235101 (2009).

[23] L. A. Constantin, J. P. Perdew, and J. M. Pitarke, Phys. Rev. B **79**, 075126 (2009).

[24] B. Wood, N. D. M. Hine, W. M. C. Foulkes, and P. García-González, Phys. Rev. B **76**, 035403 (2007).

[25] L. A. Constantin, J. M. Pitarke, J. F. Dobson, A. García-Lekue, and J. P. Perdew, Phys. Rev. Lett. **100**, 036401 (2008).

[26] See supplementary material at http://link.aps.org/supplemental/10.1103/PhysRevB.82.113104 for full results of Tables II and III.

[27] B. J. Lynch and D. G. Truhlar, J. Phys. Chem. A **107**, 8996 (2003); **108**, 1460(E) (2004).

[28] P. C. Rusu and G. Brocks, Phys. Rev. B **74**, 073414 (2006).

[29] D. Krüger, H. Fuchs, R. Rousseau, D. Marx, and M. Parrinello, J. Chem. Phys. **115**, 4776 (2001).

[30] K. Tonigold and A. Groß, J. Chem. Phys. **132**, 224701 (2010).

[31] S. D'Agostino, L. Chiodo, F. Della Sala, R. Cingolani, and R. Rinaldi, Phys. Rev. B **75**, 195444 (2007).

[32] V. Blum, R. Gehrke, F. Hanke, P. Havu, V. Havu, X. Ren, K. Reuter, and M. Scheffler, Comput. Phys. Commun. **180**, 2175 (2009).

[33] P. Haas, F. Tran, and P. Blaha, Phys. Rev. B **79**, 085104 (2009).

[34] TURBOMOLE V6, 1, University of Karlsruhe and Forschungszentrum Karlsruhe GmbH, 1989–2007, TURBOMOLE GmbH (since 2007), see http://www.turbomole.com

[35] F. Weigend and R. Ahlrichs, Phys. Chem. Chem. Phys. **7**, 3297 (2005), and references therein.